AD-A080 863 NAVAL POSTGRADUATE SCHOOL MONTEREY CA F/G 11/6
AN INVESTIGATION OF RESIDUAL STRESSES IN SIMULATED WING PANELS --ETC(U)
DEC 79 E C ENGLE

UNCLASSIFIED NL

1 OF 1
AD
A080863

END
DATE
FILMED
3 80
DTIC

(2)

NAVAL POSTGRADUATE SCHOOL

Monterey, California

LEVEL II

9 Master's THESIS

6 AN INVESTIGATION OF RESIDUAL STRESSES IN SIMULATED WING PANELS OF 7075-T6 ALUMINUM.

by

10 Edward C./Engle

11 Dec[redacted]79 12 46

Thesis Advisor: G. H. Lindsey

Approved for public release; distribution unlimited

REPORT DOCUMENTATION PAGE

READ INSTRUCTIONS BEFORE COMPLETING FORM

1. REPORT NUMBER	
2. GOVT ACCESSION NO.	
3. RECIPIENT'S CATALOG NUMBER	
4. TITLE (and Subtitle)	AN INVESTIGATION OF RESIDUAL STRESSES IN SIMULATED WING PANELS OF 7075-T6 ALUMINUM
5. TYPE OF REPORT & PERIOD COVERED	MASTER'S THESIS DECEMBER, 1979
6. PERFORMING ORG. REPORT NUMBER	
7. AUTHOR(s)	EDWARD C. ENGLE
8. CONTRACT OR GRANT NUMBER(s)	
9. PERFORMING ORGANIZATION NAME AND ADDRESS	NAVAL POSTGRADUATE SCHOOL MONTEREY, CALIFORNIA 93940
10. PROGRAM ELEMENT, PROJECT, TASK AREA & WORK UNIT NUMBERS	
11. CONTROLLING OFFICE NAME AND ADDRESS	NAVAL POSTGRADUATE SCHOOL MONTEREY, CALIFORNIA 93940
12. REPORT DATE	DECEMBER, 1979
13. NUMBER OF PAGES	45
14. MONITORING AGENCY NAME & ADDRESS (if different from Controlling Office)	NAVAL POSTGRADUATE SCHOOL MONTEREY, CALIFORNIA 93940
15. SECURITY CLASS. (of this report)	UNCLASSIFIED
15a. DECLASSIFICATION/DOWNGRADING SCHEDULE	

16. DISTRIBUTION STATEMENT (of this Report)

APPROVED FOR PUBLIC RELEASE; DISTRIBUTION UNLIMITED

17. DISTRIBUTION STATEMENT (of the abstract entered in Block 20, if different from Report)

APPROVED FOR PUBLIC RELEASE; DISTRIBUTION UNLIMITED

18. SUPPLEMENTARY NOTES

NONE

19. KEY WORDS (Continue on reverse side if necessary and identify by block number)

Residual Stress, Stress Concentration, Strain Concentration

20. ABSTRACT (Continue on reverse side if necessary and identify by block number)

The advent of onboard aircraft microprocessor fatigue monitoring systems will establish the opportunity to fully exploit residual stresses at stress-critical areas, including their effects on fatigue predictions. An experimental investigation was undertaken to more fully understand them by making photoelastic measurements of residual stresses at notches in simulated wing

BLOCK 20. ABSTRACT (Cot'd.)

panels of 7075-T6 aluminum and to establish the relationships between local stresses, residual stresses, and the far-field or applied stress. The stress concentration factors were found to decrease with increased plastic deformation while the strain concentration factors were found to remain constant. The residual stress levels were found to be immutable despite changes in fatigue loading conditions, notch geometry, or test duration.

Approved for public release; distribution unlimited

An Investigation of Residual Stresses In Simulated Wing Panels of 7075-T6 Aluminum

by

Edward C. Engle

Lieutenant Commander, United States Navy
B.E.S., The Johns Hopkins University, 1966

Submitted in partial fulfillment of the requirements for the degree of

MASTER OF SCIENCE IN AERONAUTICAL ENGINEERING

from the

UNITED STATES NAVAL POSTGRADUATE SCHOOL

December 1979

Author: Edward C. Engle

Approved by: ______________________ Thesis Advisor

______________________ Chairman, Department of Aeronautics

______________________ Dean of Science and Engineering

ABSTRACT

The advent of onboard aircraft microprocessor fatigue monitoring systems will establish the opportunity to fully exploit residual stresses at stress-critical areas, including their effects on fatigue predictions. An experimental investigation was undertaken to more fully understand them by making photoelastic measurements of residual stresses at notches in simulated wing panels of 7075-T6 aluminum and to establish the relationships between the local stresses, residual stresses, and the far-field or applied stress. The stress concentration factors were found to decrease with increased plastic deformation while the strain concentration factors were found to remain constant. The residual stress levels were found to be immutable despite changes in fatigue loading conditions, notch geometry, or test duration.

Table of Contents

List of Figures

ACKNOWLEDGEMENT

I wish to express my appreciation to Professor G. H. Lindsey for his assistance in the preparation of this paper and his guidance in the conduct of the experiments, especially when unforeseen difficulties arose.

I. INTRODUCTION

With the advent of microprocessor-type fatigue monitors, new in-flight recorded information will be forthcoming with which, it is hoped, more accurate cumulative damage calculations can be made. Newly-available information will include sequence of loading and minimum values of each cycle as well as maximum values, which have been available for some time. With these two kinds of data being collected, it is appropriate to make inquiry into the influence they have upon fatigue life. One of the ways that the load sequence exerts an influence is through the residual stress that is produced at a site of stress concentration.

When a notched specimen has been subjected to nominal stresses below the yield point of the material far removed from the notch, it is possible for that area at the tip of the notch to yield due to the concentration of stress at that point. Then, upon unloading, the surrounding material compresses the locally-yielded area resulting in a residual compressive stress, which has been shown to increase the fatigue life of the specimen [1, 2, 3].

Local stresses and residual stresses must be calculated from a knowledge of the prevailing nominal stresses, which are those stresses which would be present if there were no stress concentration: in other words, those stresses that are present which are out of the influence of the notch. It is the nominal stress that will be determined from the in-flight fatigue monitors.

It was the purpose of this thesis to use photoelastic methods to measure residual stresses in typical notches of simulated wing panels

and to relate the residual stress and the local stress to the applied nominal stress.

Classically, Neuber's relationship [4] has been used in such calculations; but Garske [5] found considerable error with the method in some instances, establishing the need for more accurate analyses.

Stuart [6] used photoelastic coatings on notched plate specimens to establish the relationship between cyclic loading and residual stress levels. He found in preliminary tests that the residual stress *vs.* nominal stress curves could be used to predict the residual stress to within 10% of the measured stress and that once induced, the residual stress was constant during low-cycle fatigue tests at a relatively high stress level. Knowing the value of the residual stress, it would be possible to use the aircraft-mounted microprocessor output to simulate conditions at the notch, or stress-critical area, by reducing the applied load an amount equivalent to the residual stress induced by the highest previously-encountered load.

An experimental investigation of the residual stress and its influence on conditions at the notch was made as a continuation of Stuart's work, using the same notched specimens. Again, photoelastic coatings were used for fatigue testing instead of strain gauges because of the relatively poor fatigue performance of the latter. Strain gauges were used, however, in certain of the static tests.

II. EXPERIMENTAL PROCEDURE

A. SPECIMEN DESCRIPTION

The notched aluminum sheet specimens were the same ones used by Stuart [6]. They were fabricated from 0.080 inch thick 7075-T6 aluminum in 1' x 4' sheets. Two different notch geometries were used (see Figure 1) with nominal stress concentration factors of 2.60 and 3.80. PS-1C photoelastic material, by Photoelastic, Inc., was bonded to the specimens with PC-1 cement. The photoelastic material was designed for use on high-modulus materials like 7075 and for maximum elongations up to 10%. The bonding agent allowed maximum elongations of 3-5%.

Uniaxial tensile test specimens were made from 0.090 inch thick 7075-T6 aluminum sheets in two configurations (see Figure 2); one had a reduced section over the gauge length while the other was uniform.

Strain gauges were mounted on some specimens as shown in Figure 2. The gauges used were EP-08-060CN-120 by Micro Measurements. These gauges were specifically designed for use in the measurement of plastic strains of from 7-10% but were not recommended for fatigue applications.

B. CHARACTERIZATION OF THE 7075-T6 ALUMINUM

1. Young's Modulus

Specimen types A and B (see Figure 2) were both used in the determination of Young's Modulus. The A-type specimens were run on the Riehle machine while the B-type were run on the MTS machine. One of the B-type specimens was instrumented with an MTS 632.13B-20 extensometer on its longitudinal axis in addition to the strain gauge, and a linear

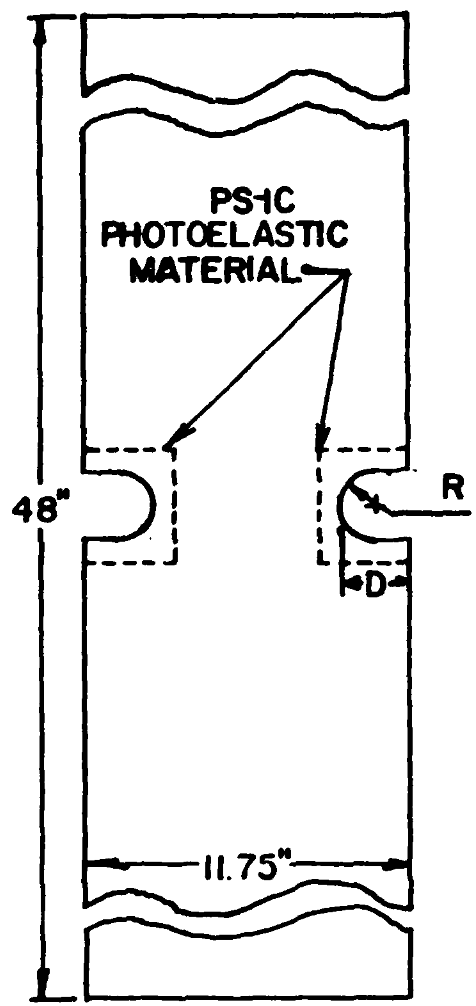

SPECIMEN GEOMETRIES

NOMINAL K_T	2.6	3.8
R (in)	0.900	0.3125
D (in)	1.415	1.963
REDUCED CROSS-SECTION (in^2)	0.7136	0.626

NOTES:

1. 7075-T6 ALUMINUM
2. THICKNESS = 0.080 in

FIGURE 1

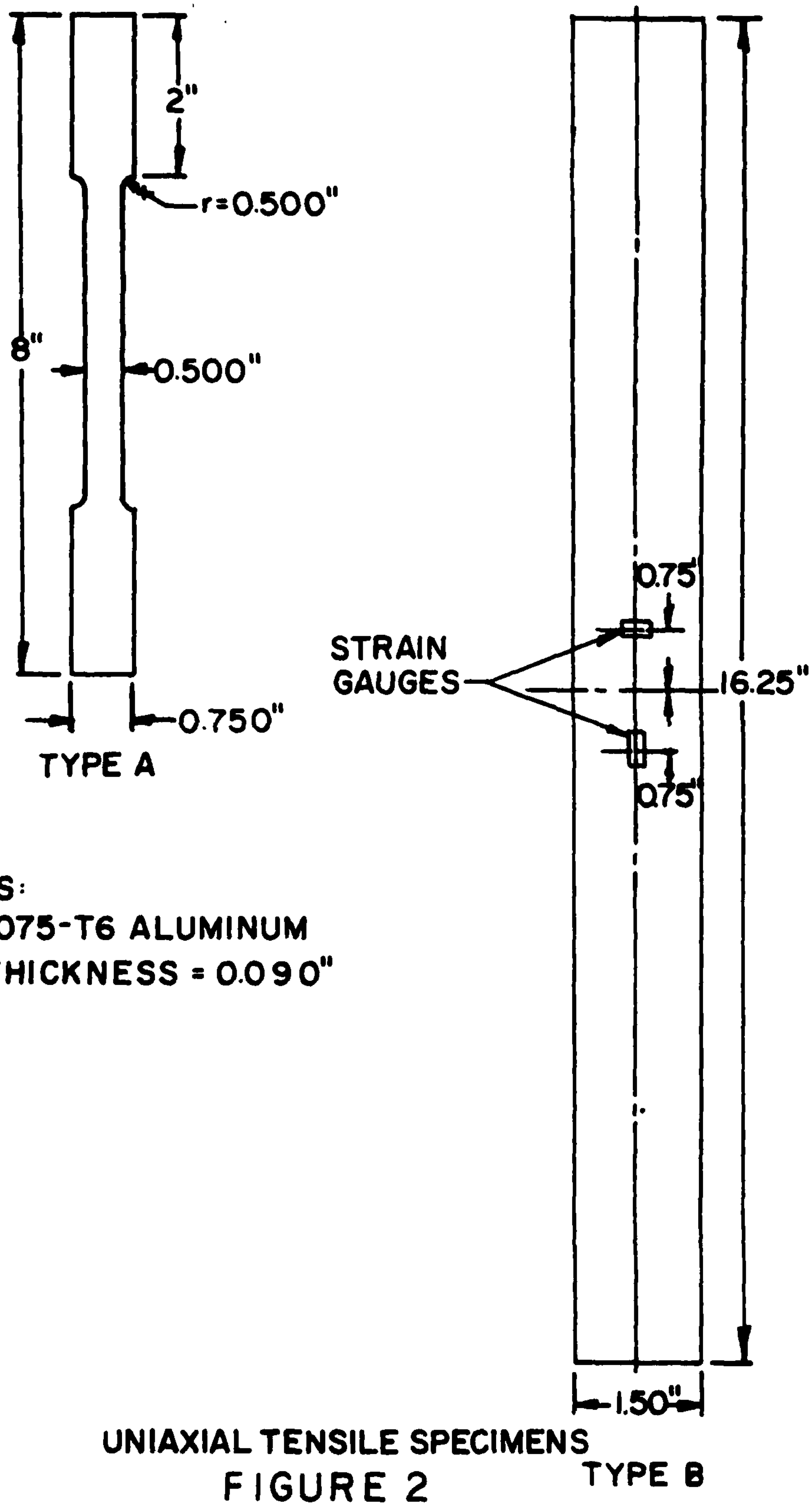

NOTES:
1. 7075-T6 ALUMINUM
2. THICKNESS = 0.090"

UNIAXIAL TENSILE SPECIMENS
FIGURE 2

regression analysis was performed to determine Young's Modulus. The extensometer yielded $E = 9.915 \times 10^6$ psi with a correlation coefficient of 0.999916, while the strain gauge yielded $E = 10.11 \times 10^6$ psi with a correlation coefficient of 0.999994 (see Table 1 of Appendix A). Although the values were within 2% of each other, it was decided to use the latter because it had a slightly better correlation coefficient and is in better agreement with the literature.

Due to the small size of the specimen, the largest scale available on the Riehle machine proved to be too small to accurately determine Young's Modulus (values of $E = 9.7 \times 10^6$ to 9.9×10^6 were generated). However, since repetitive tests were run on each of the A-type specimens into the plastic region, it was established that the unloading curve matched the loading curve (see Figure 3). Figure 4 is a graphical representation of the results of the static tensile tests. The residual strain remaining at the final no-load condition of the specimen was 12,678 μs. This provided a value of Young's Modulus for unloading of:

$$E = \frac{81.620-0.000 \text{ (ksi)}}{20,896-12,678 \ (\mu s)}$$

$$E = 9.93 \times 10^6 \text{ psi}$$

The measured values of Young's Modulus from the loading portion of the static tensile tests established a disagreement level given by:

$$\frac{10.11-9.915}{10.11} \times 100\% = 1.9\% \quad ,$$

whereas the value measured during unloading yielded a disagreement of

$$\frac{10.11-9.93}{10.11} \times 100\% = 1.8\% \quad ,$$

STRESS - STRAIN CURVES FOR REPETITIVE LOADING

FIGURE 3

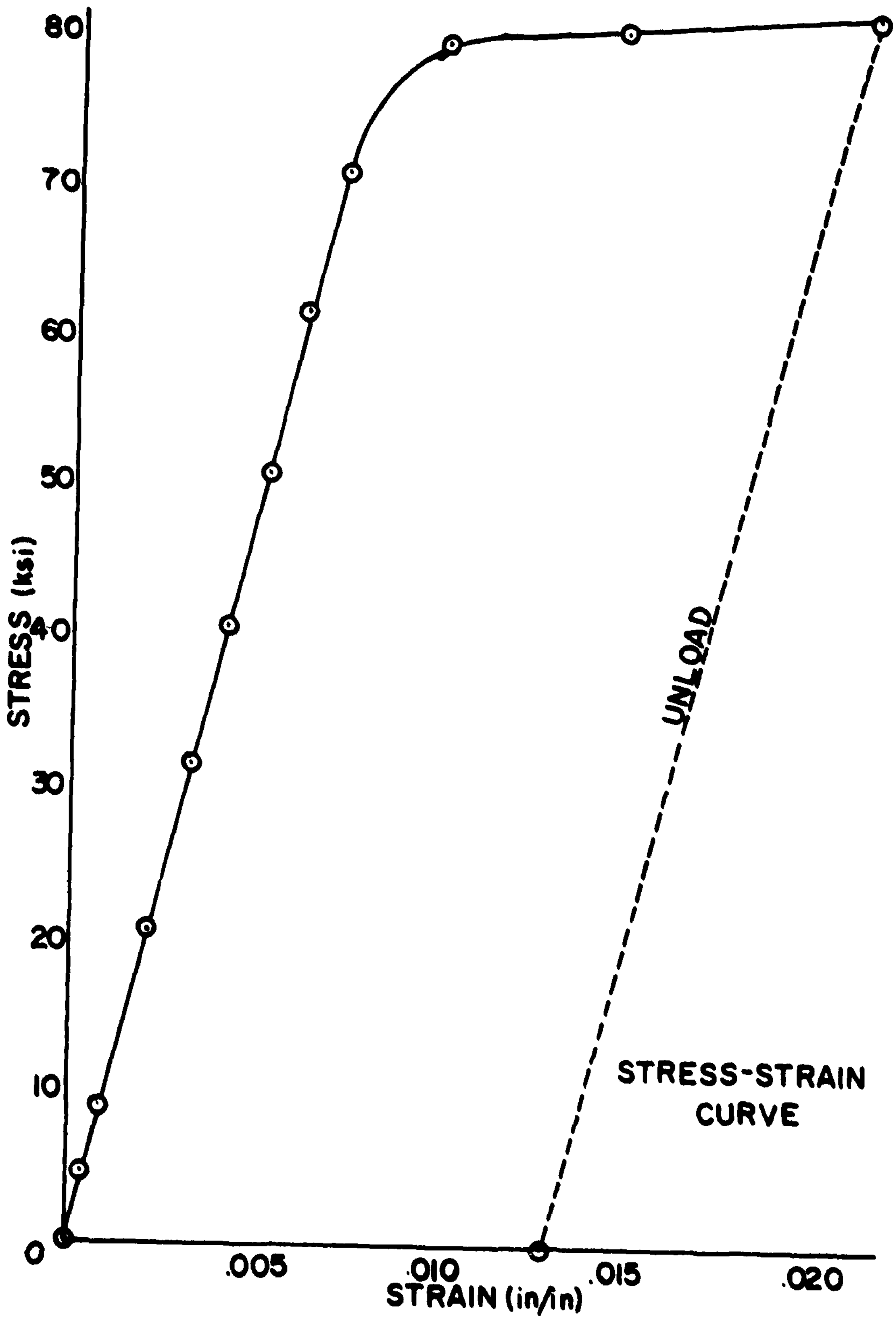
80
70
60
50
40
30
20
10
0
STRESS (ksi)
.005
.010
.015
.020
STRAIN (in/in)
UNLOAD
STRESS-STRAIN
CURVE
FIGURE 4

within the uncertainty in the measurement of the strain in the static tensile test itself.

2. Poisson's Ratio

The B-type specimen was used to determine Poisson's Ratio. The geometry was developed in accordance with ASTM standards. Extensometers were not used because an extensometer suitable for mounting in the transverse direction was not available. (Since the objective of the experiment was to trace the changes in Poisson's Ratio well into the plastic region, use of a single extensometer and two separate test runs was precluded). Hence, strain gauges were used in conjunction with a longitudinally-mounted extensometer (see Table 2 of Appendix A for data). Corrections were made for transverse effects on the transverse strain gauge. In neither test was Poisson's Ratio observed to shift from 0.3 to 0.5 as dictated by the plastic behavior of a constant-volume specimen (see Figures 5 and 6).

3. Yield and Plastic Behavior

The slopes of the various stress-strain curves generated were very flat above the elastic limit showing almost perfectly plastic behavior. For a plastic, constant-volume material, the sum of the principal strains must be zero--that is, $\varepsilon_1+\varepsilon_2+\varepsilon_3 = 0$. Substituting in terms of Poisson's ratio, for a uniaxial specimen,

$$-\nu\varepsilon_3-\nu\varepsilon_3+\varepsilon_3 = 0 \quad .$$

Or,

$$\varepsilon_3(1 - 2\nu) = 0 \quad .$$

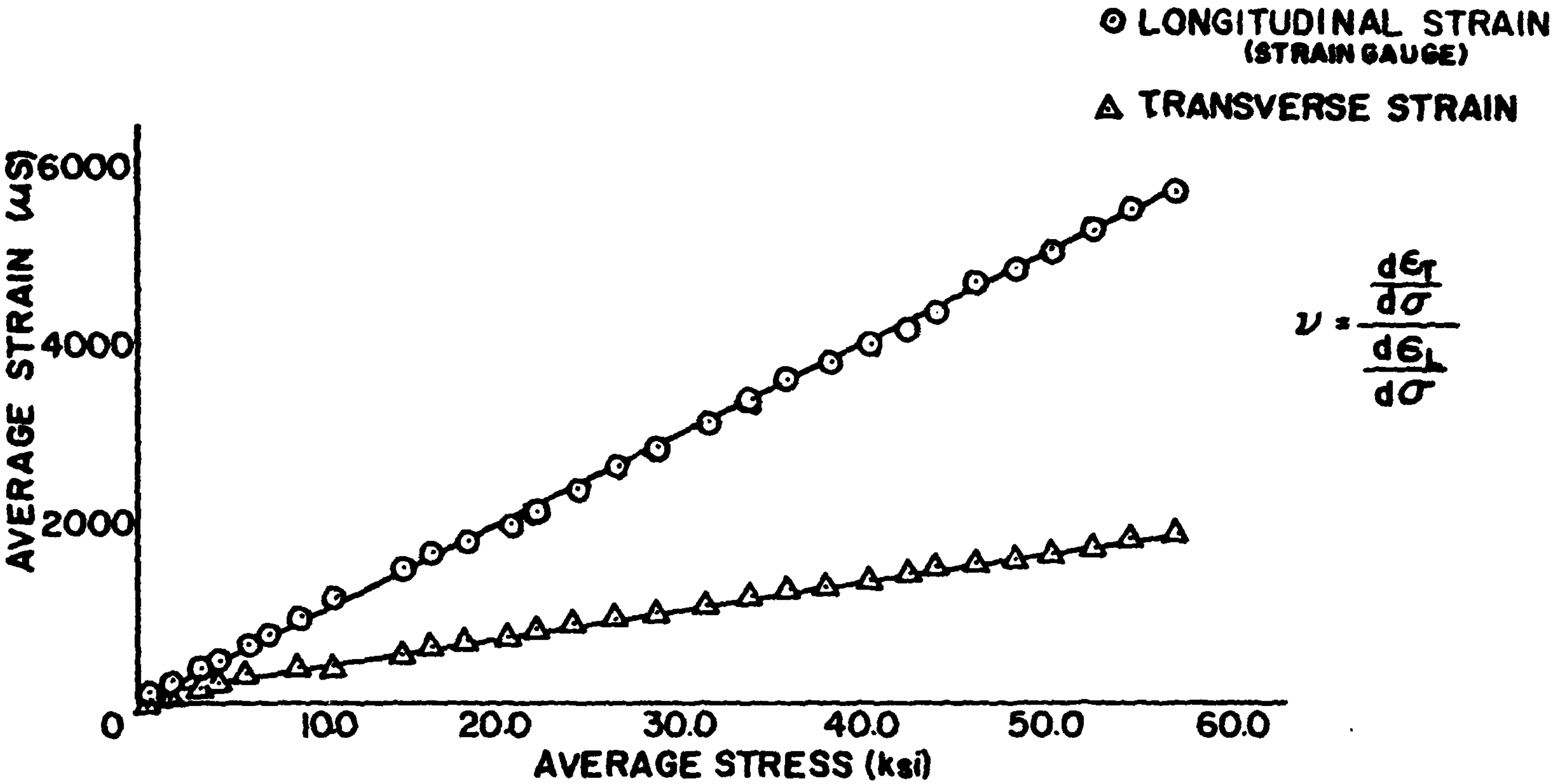

AVERAGE STRESS VS. AVERAGE STRAINS FOR DETERMINATION OF POISSON'S RATIO (ELASTIC RANGE)

FIGURE 5

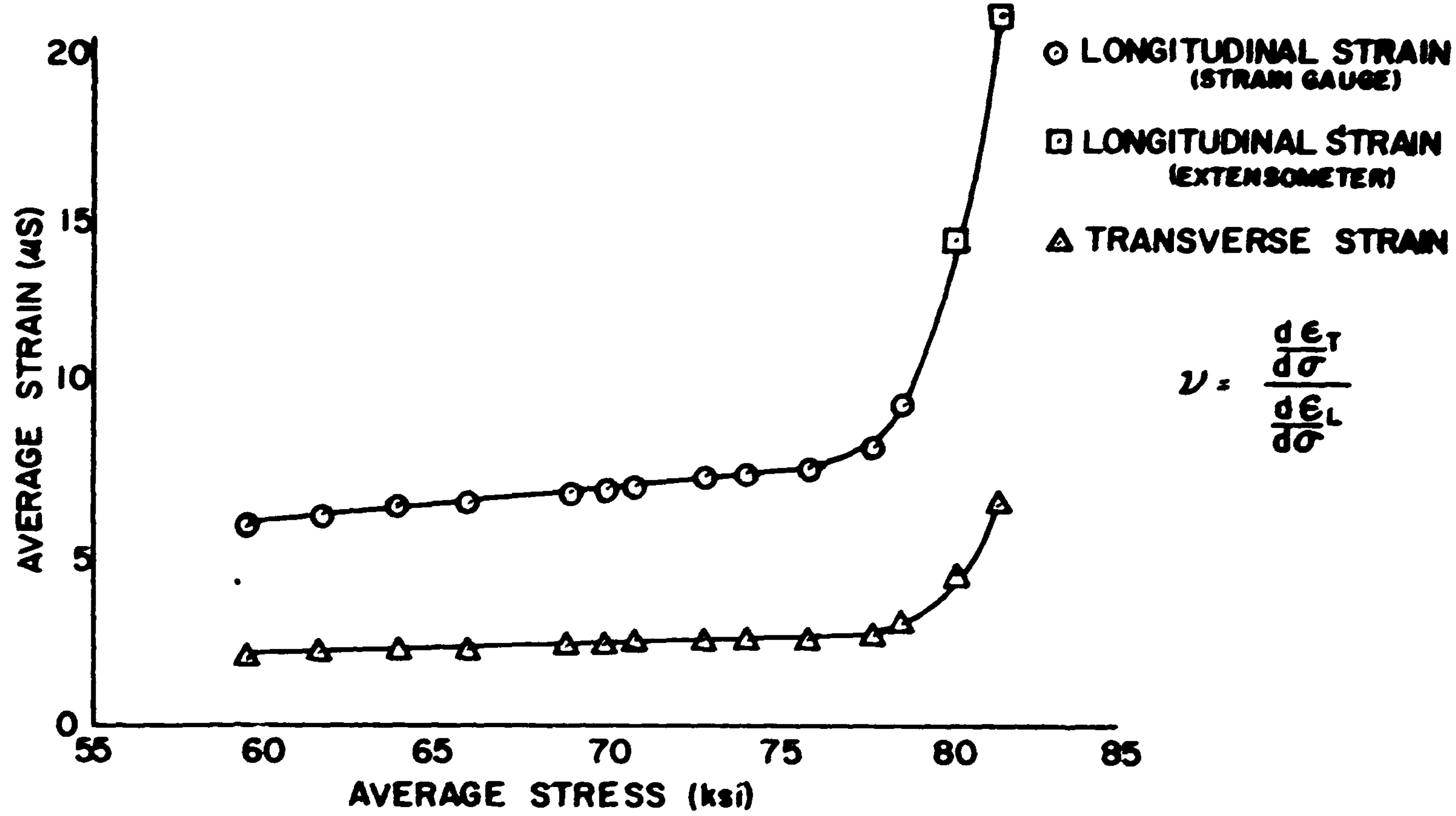

AVERAGE STRESS VS. AVERAGE STRAINS FOR DETERMINATION OF POISSON'S RATIO (PLASTIC RANGE)

FIGURE 6

Hence, $\nu = \frac{1}{2}$. As stated above, this phenomenon could not be verified for strain levels up to 2%.

C. CHARACTERIZATION OF PS-1C PHOTOELASTIC MATERIAL

A uniaxial tensile test specimen was prepared from a sheet of PS-1C photoelastic material and loaded in a test machine. Compensator readings were taken at the same load levels at the extensometer readings, and the data in Table 3 of Appendix A was generated.

1. Strain Optic Coefficient (α)

A linear regression analysis of the strain-compensator data yielded

$$\varepsilon = 0.0012362N + 0.00000996 \tag{1}$$

$$r^2 = 0.9989 \quad .$$

Discarding the non-zero intercept, since it is three orders of magnitude smaller than the strain levels, equation (1) yielded

$$\frac{d\varepsilon}{dN} = \alpha = 0.0012362 \quad . \tag{2}$$

2. Young's Modulus

A separate linear regression analysis of the stress-strain data yielded

$$\sigma = 358{,}043\varepsilon - 139.6 \tag{3}$$

$$r^2 = 0.9989 \quad .$$

Discarding the non-zero intercept as being small compared to the range of the stress, equation (3) yielded E = 358,043 psi. Photoelastic, Inc., advertised E = 360,000 psi, nominal.

From [7],

$$\varepsilon_x - \varepsilon_y = \frac{\lambda}{2tk}N \quad ,$$

where λ = the wavelength of the light source (22.7×10^{-6} in.)

t = thickness of the photoelastic material (0.040 in.)

N = fringe order number

k = sensitivity of the plastic (0.15)

Solving for ε_x in terms of Poisson's Ratio for a uniaxial field,

$$\varepsilon_x = \frac{\lambda}{(1+\nu)2tk}N \quad . \tag{4}$$

From equation (2),

$$\alpha = \frac{\lambda}{(1+\nu)2tk} \quad . \tag{5}$$

Solving equation (5) for Poisson's Ratio,

$$\nu = \frac{\lambda}{2tk\alpha} - 1 \quad . \tag{6}$$

Substituting numerical values into equation (6), $\nu = 0.5302$, which cannot be. Therefore, since t and α were measured, and the value for λ is generally accepted in the literature, it was concluded that the k value given by the vendor was in error, and the measured value of α was used in the data reduction.

D. EXPERIMENTAL DETERMINATION OF STRESS CONCENTRATION FACTOR (K_T)

Stuart determined the individual stress concentration factors for each specimen experimentally [6] by the following method, which models the notch tip as a uniaxial specimen:

Multiplying equation (4) by E, the notch stress below the elastic limit can be written

$$\sigma_N = \frac{E}{(1+\nu)} \cdot \frac{\lambda}{2tk} N = E\alpha N \quad .$$

If the nominal stress (σ) is defined as the applied load divided by the reduced cross-sectional area, the stress concentration factor is

$$K_T = \frac{\sigma_N}{\sigma} \quad .$$

By loading the specimen to a known point elastically and then recording the compensator reading, Stuart was able to establish both the nominal stress and the fringe order number at the notch. Hence, K_T could be determined experimentally. These values were used in the analysis.

E. EXPERIMENTAL DETERMINATION OF STRAIN CONCENTRATION FACTOR (K_ε)

Similar to the stress concentration factor, the strain concentration factor can be determined. The notch strain can be found from equation (4):

$$\varepsilon_N = \frac{\lambda}{(1+\nu)2tk} N = \alpha N$$

Then, if we define the nominal strain (ε) as the nominal stress (σ) divided by Young's Modulus, the strain concentration factor is

$$K_\varepsilon = \frac{\varepsilon_N}{\varepsilon} \quad .$$

By using Stuart's σ_{MAX} data and σ_{MAX} data established in this thesis at 18.00 kips (*cf.* III., RESIDUAL STRESS MEASUREMENTS), it was possible to formulate values of K_ε at two different loading conditions.

III. RESIDUAL STRESS MEASUREMENTS

A. UNIAXIAL MODEL

The model used in this study is described schematically in Figure 7. The specimen was loaded until the material at the notch exceeded the elastic limit (the remainder of the specimen was still elastic because of the effect of stress concentration). Unloading caused the region at the notch to be placed in a state of compressive residual stress and tensile residual strain. The unloading curve was at the same slope as the loading curve (Young's Modulus was constant). Subsequent reloadings began from this residual state with the material exhibiting the same value of Young's Modulus as all previous loadings/unloadings. The value of the residual stress, σ_R, was, from the geometry of Figure 7,

$$\sigma_R = \sigma_{MAX} - E(\epsilon_{MAX} - \epsilon_R) \quad , \tag{7}$$

where σ_{MAX} = maximum stress to which the notch was exposed

ϵ_{MAX} = maximum strain to which the notch was exposed

ϵ_R = residual tensile strain.

Subsequent values of the notch stress were then given by

$$\sigma_{NOTCH} = E(\epsilon_{NOTCH} - \epsilon_R) + \sigma_R \quad , \tag{8}$$

where σ_{NOTCH} = notch stress subsequent to initial loading to σ_{MAX}

ϵ_{NOTCH} = notch strain subsequent to initial loading to σ_{MAX}.

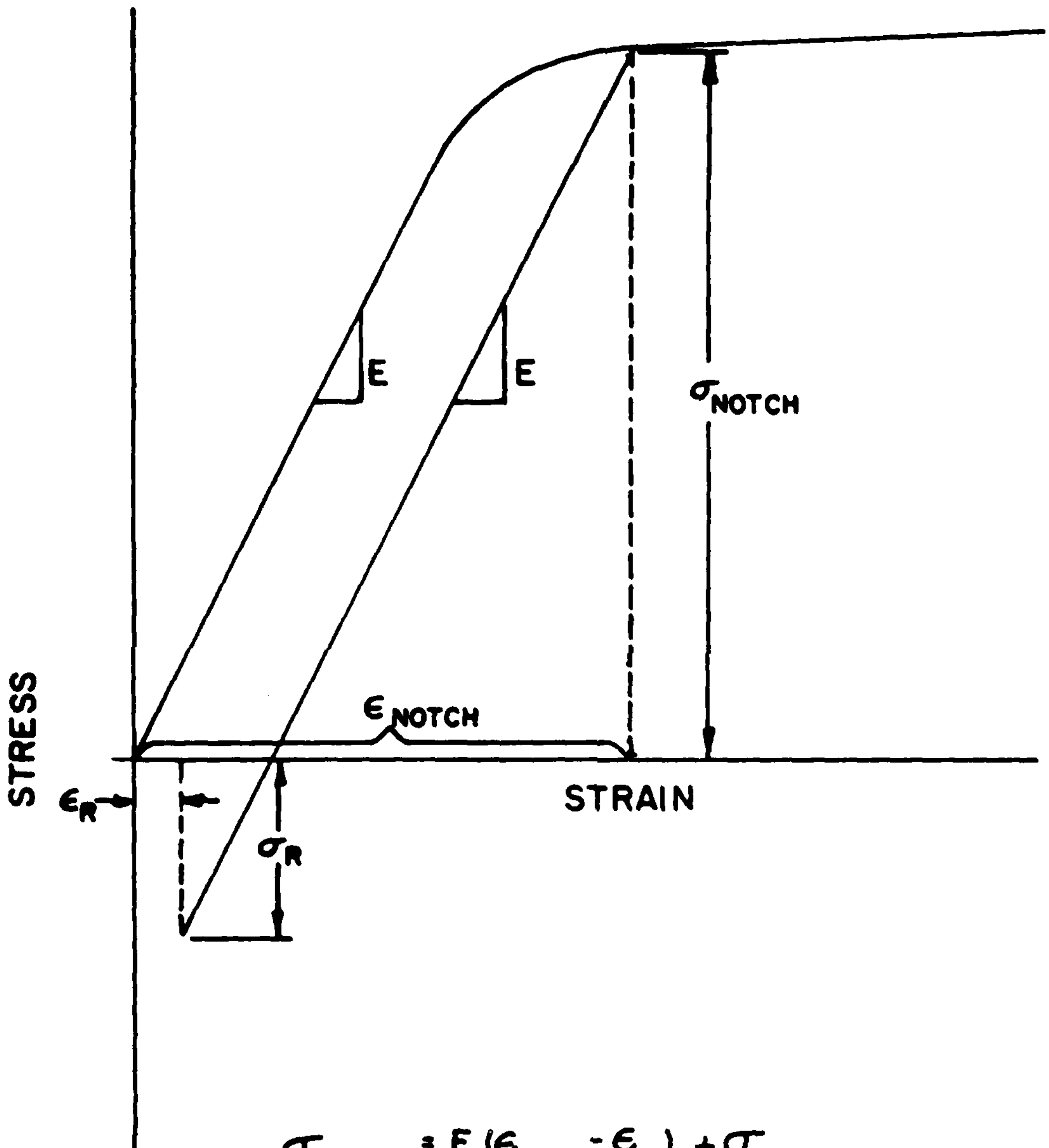

$$\sigma_{NOTCH} = E(\epsilon_{NOTCH} - \epsilon_R) + \sigma_R$$

RESIDUAL STRESS MODEL

FIGURE 7

Classically, the value of the stress at the notch can be calculated in the elastic region if the far-field loading, the cross-sectional area, and the stress concentration factor are known:

$$\sigma_{NOTCH} = K_T \cdot \frac{P_{FF}}{A} \quad , \tag{9}$$

where P_{FF} = the far-field load

A = the reduced cross-sectional area.

If there is a residual stress present, it changes σ_{NOTCH} linearly (see Figure 7). Therefore, equation (9) would become

$$\sigma_{NOTCH} = K_T \cdot \frac{P_{FF}}{A} + \sigma_R \quad . \tag{10}$$

B. EVALUATIVE TESTS

Since specimens 1, 3, and 7 (nominal K_T = 3.8) had only been loaded by Stuart to 13.60, 14.00, and 14.00 kips, respectively, they were chosen to verify the uniaxial model since they could be loaded to 18.00 kips, and thus establish a new value for σ_{MAX}. Other available specimens had already been exposed to high loads and, therefore, the previously-derived values of σ_{MAX} obtained by Stuart's photoelastic readings would have had to be used--deleting an element of operator consistency from the experiment.

Initially, no-load compensator readings were taken of all three specimens previously tested by Stuart, which were to evaluate any decay in residual strain which may have occurred. Only specimen 3 correlated with Stuart's work (see Table 4, Appendix A). No fringes at all could be observed on specimen 7, and only one of the notches on specimen 1 showed any fringe value, which was almost 3 times higher than Stuart's. Other

specimens tested by Stuart were then read photoelastically in an effort to verify Stuart's residual compensator readings, but the data proved inconclusive (see Table 4, Appendix A). Three specimens yielded markedly lower compensator readings, four specimens yielded markedly greater compensator readings, and one specimen yielded one higher (left notch) and one lower (right notch) compensator readings than reported in [6]. Several readings were taken on each specimen and were always within a few points of each other. Therefore, the data was repeatable; and the reason for the disagreement was unknown.

Returning to specimens 1, 3, and 7, each was loaded to 18.00 kips, and the fringe values at maximum and no-load conditions were recorded as listed in Table 5 of Appendix A. Values of ε_{MAX} and ε_R could be derived for a particular fringe by use of equation (4). The corresponding value of σ_{MAX} was found by referring to the uniaxial stress-strain data generated in the static tests while σ_R was calculated from equation (7), developed from the model (see Table 7, Appendix A).

In order to establish the immutability of the residual stress, specimens 6, 8, 9, 10, and 11 (nominal $K_T = 3.8$) and specimens 7, 13, and 14 (nominal $K_T = 2.6$) were tested in fatigue under various loading conditions in the MTS machine (see Table 6, Appendix A for the load ranges used). The no-load condition compensator readings were recorded periodically during the tests. Each of these specimens had been tested previously by Stuart and had various residual notch stress levels already induced [6]. These readings corresponded to the residual strain level which, by substitution into equations (4) and (7), fixed the value of the residual stress at the notch. Table 6 of Appendix A summarizes the results. Generally, the compensator readings tended to remain constant throughout

the tests regardless of specimen geometry, residual stress condition, or load levels.

Prior to performing any further fatigue tests, it was necessary to verify the stress levels predicted by equation (10), because these were the values which were to be used to set the loading limits on the MTS machine for the cyclic tests. Hence, each specimen (1, 3, and 7) was loaded in 500-lb. increments to 5.00 kips far-field load and the compensator readings recorded at each level. Knowing σ_{MAX}, σ_R, K_T, A, and N, the predictions made by equation (10) could be compared with the actual values given by equation (8). Figures 8-12 illustrate the poor agreement between the predictions of equation (10) and the results of equation (8) using data obtained from the compensator readings recorded at each level.

Using a wide rectangular block (plane strain) with two uniform semicircular notches, Hill [8] showed in 1948 that initial yielding occurred at the point of greatest notch curvature (the tip); but, as the applied end loading was increased, the plastic spread, and "the plastic-elastic boundary was a curve along which the maximum shear stress was constant." Furthermore, the stress concentration was dissipated by the local plastic flow (the remainder of the material being elastic). Therefore, since equation (10) utilized the initial value of K_T as measured by Stuart, the value of σ_{NOTCH} thus calculated should have been higher than physically present due to the reduction in K_T with increased loading. Figures 8-12 show this to be the case. Linear regression analyses were performed on the data to establish the reduced value of K_T. The results are tabulated in Table 7 of Appendix A and show an average reduction in K_T of 23.9% (minimum of 20.6% and maximum of 28.9%).

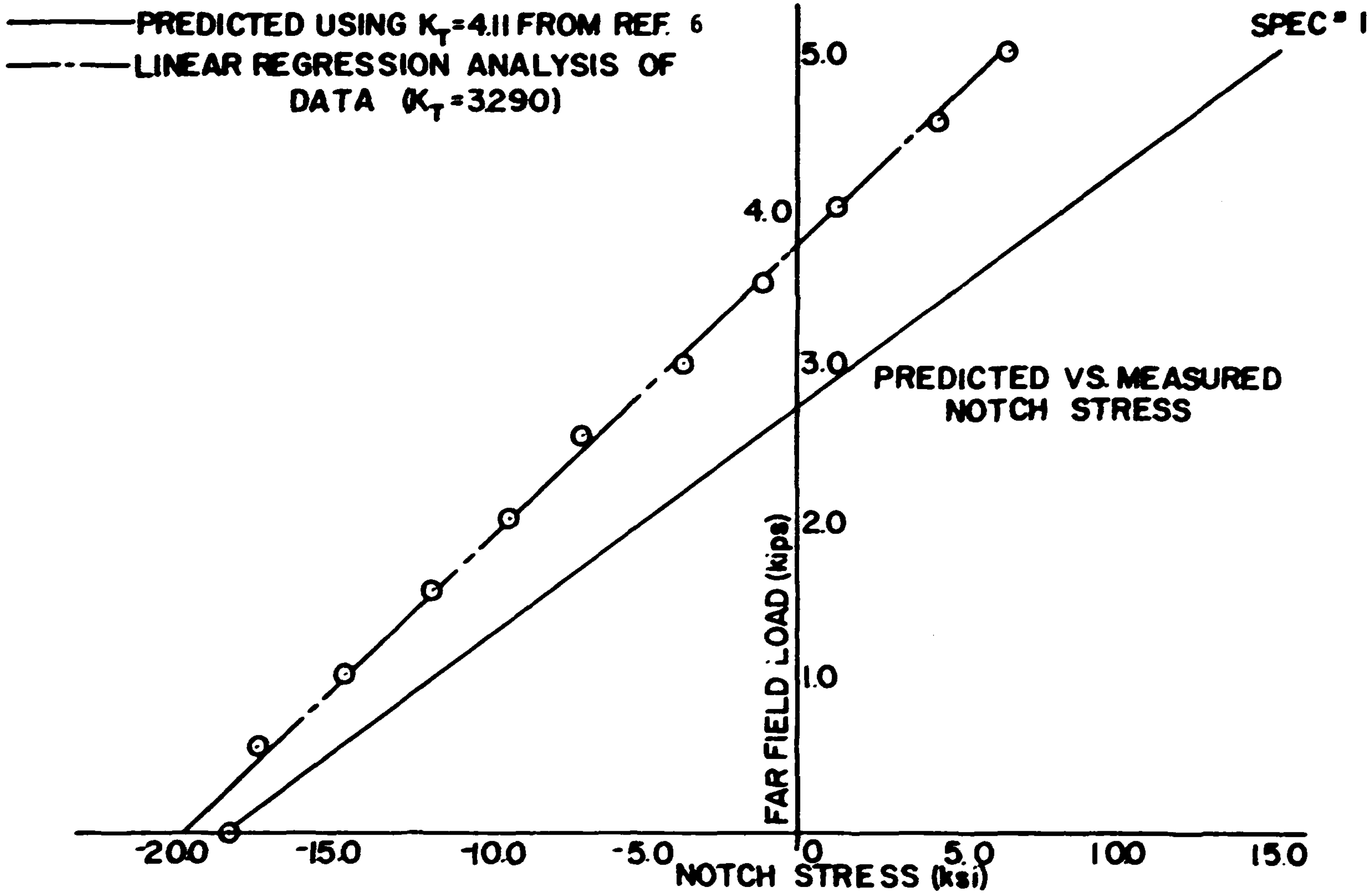
PREDICTED USING K_T=4.11 FROM REF. 6
LINEAR REGRESSION ANALYSIS OF DATA (K_T=3290)
SPEC# 1
PREDICTED VS. MEASURED NOTCH STRESS
FAR FIELD LOAD (kips)
NOTCH STRESS (ksi)
5.0
4.0
3.0
2.0
1.0
-20.0
-15.0
-10.0
-5.0
0
5.0
10.0
15.0

FIGURE 8

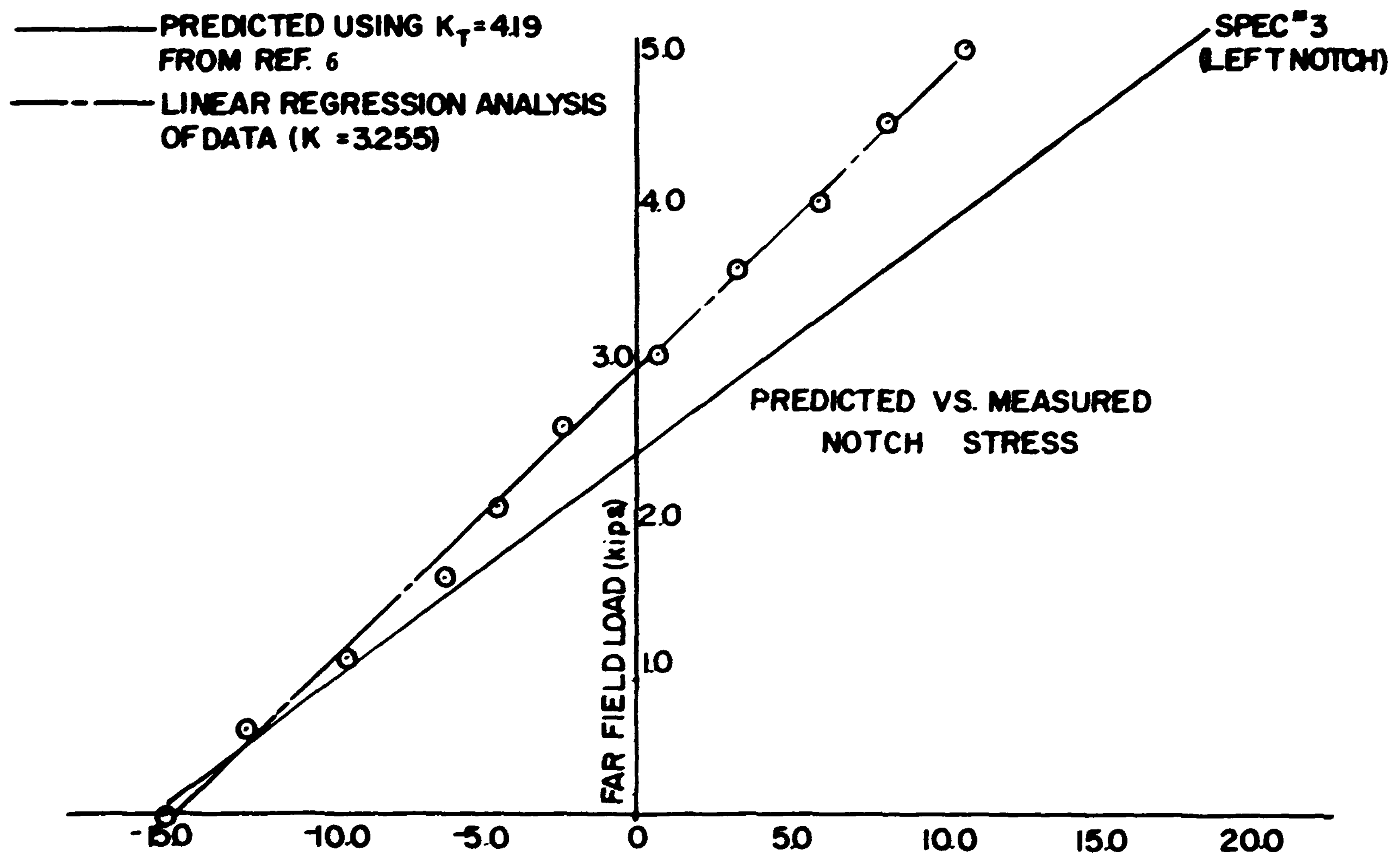
PREDICTED USING K_T=4.19
FROM REF. 6
LINEAR REGRESSION ANALYSIS
OF DATA (K =3.255)
SPEC #3
(LEFT NOTCH)
PREDICTED VS. MEASURED
NOTCH STRESS
FAR FIELD LOAD (kips)
5.0
4.0
3.0
2.0
1.0
-15.0
-10.0
-5.0
0
5.0
10.0
15.0
20.0

FIGURE 9

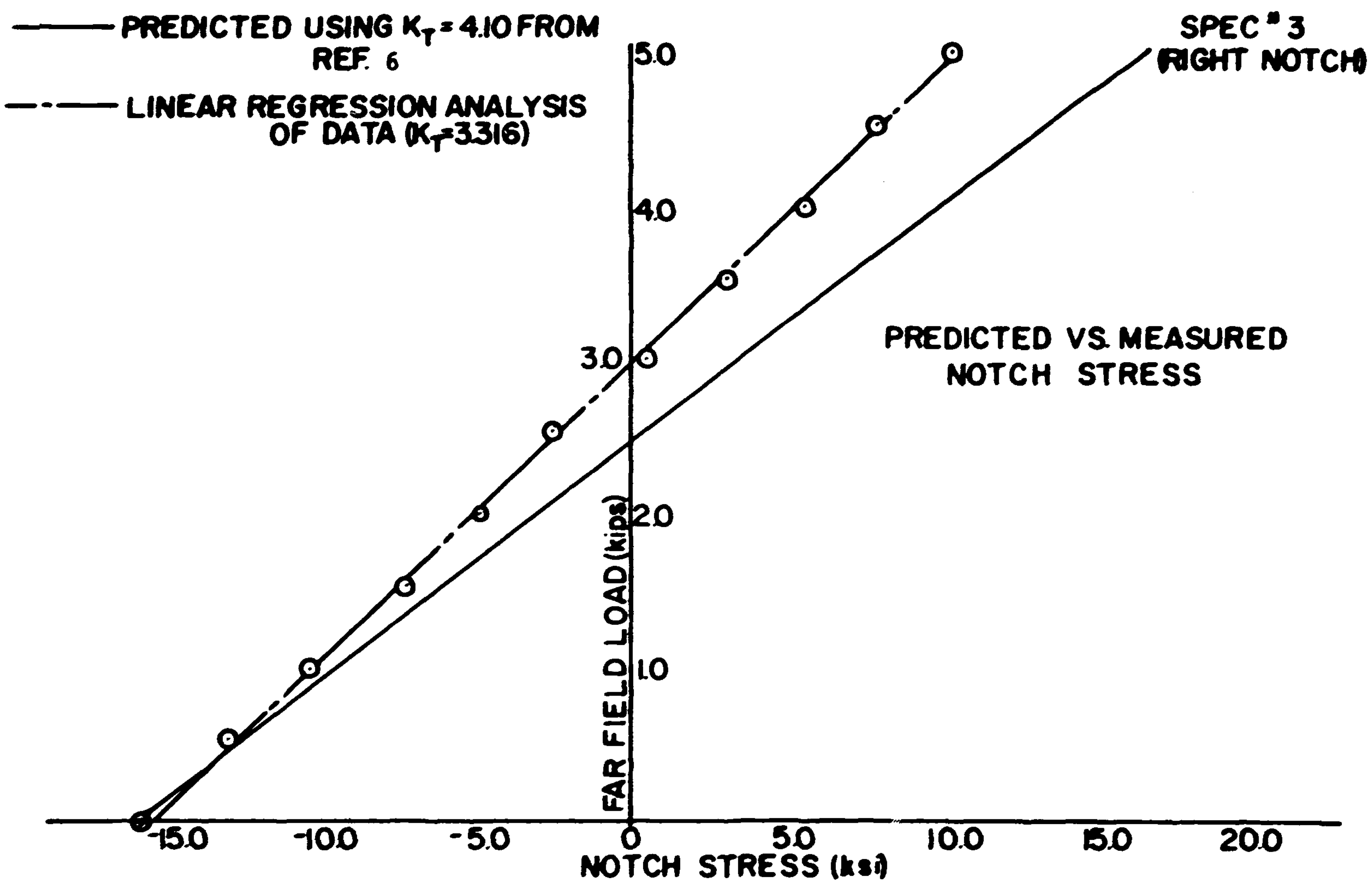
PREDICTED USING K_T = 4.10 FROM REF. 6
LINEAR REGRESSION ANALYSIS OF DATA (K_T=3.316)
SPEC # 3 (RIGHT NOTCH)
PREDICTED VS. MEASURED NOTCH STRESS
FAR FIELD LOAD (kips)
5.0
4.0
3.0
2.0
1.0
-15.0
-10.0
-5.0
0
5.0
10.0
15.0
20.0
NOTCH STRESS (ksi)

FIGURE 10

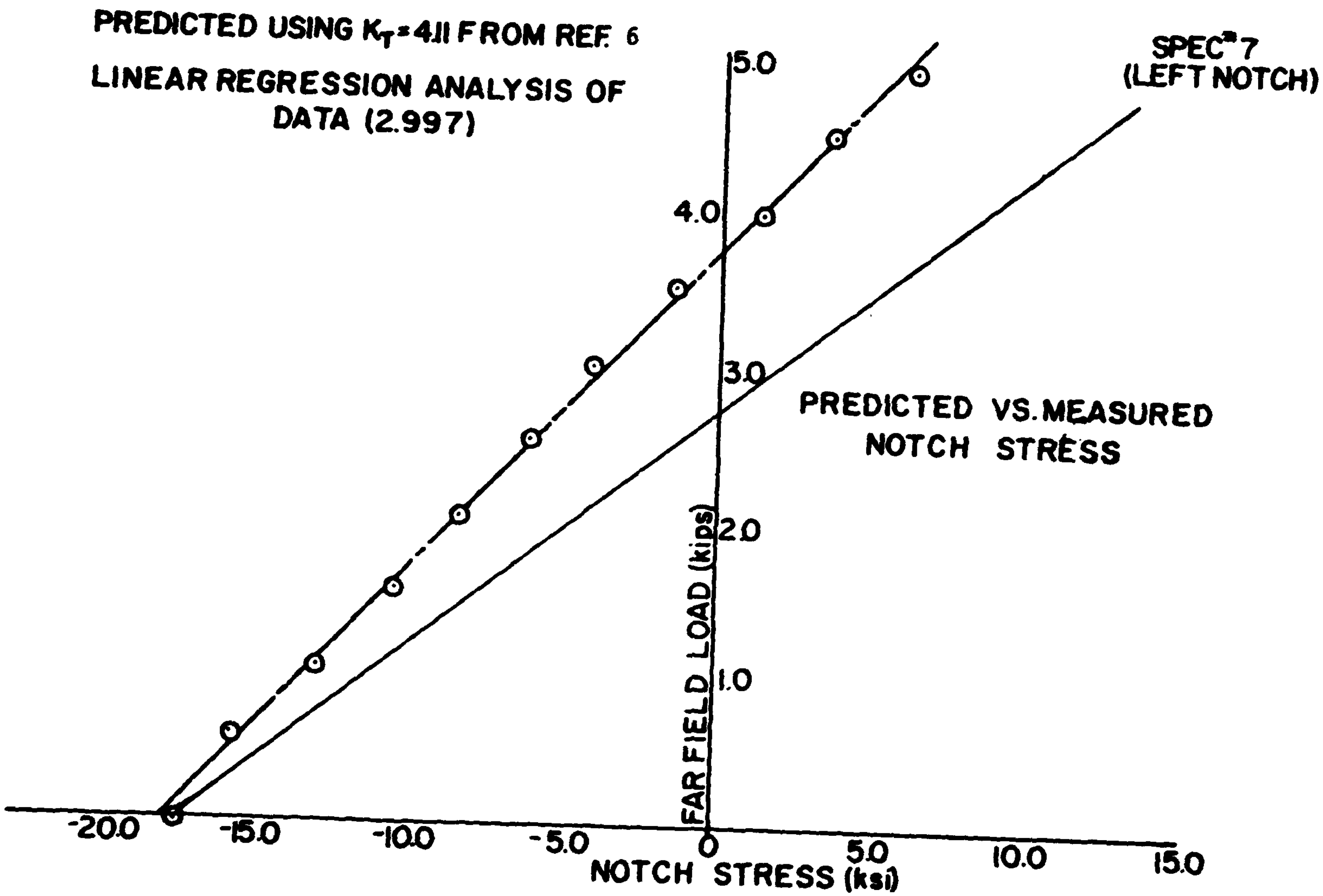
PREDICTED USING $K_T = 4.11$ FROM REF. 6
LINEAR REGRESSION ANALYSIS OF DATA (2.997)
SPEC. # 7 (LEFT NOTCH)
PREDICTED VS. MEASURED NOTCH STRESS
FAR FIELD LOAD (kips)
1.0
2.0
3.0
4.0
5.0
-20.0
-15.0
-10.0
-5.0
0
5.0
10.0
15.0
NOTCH STRESS (ksi)

FIGURE 11

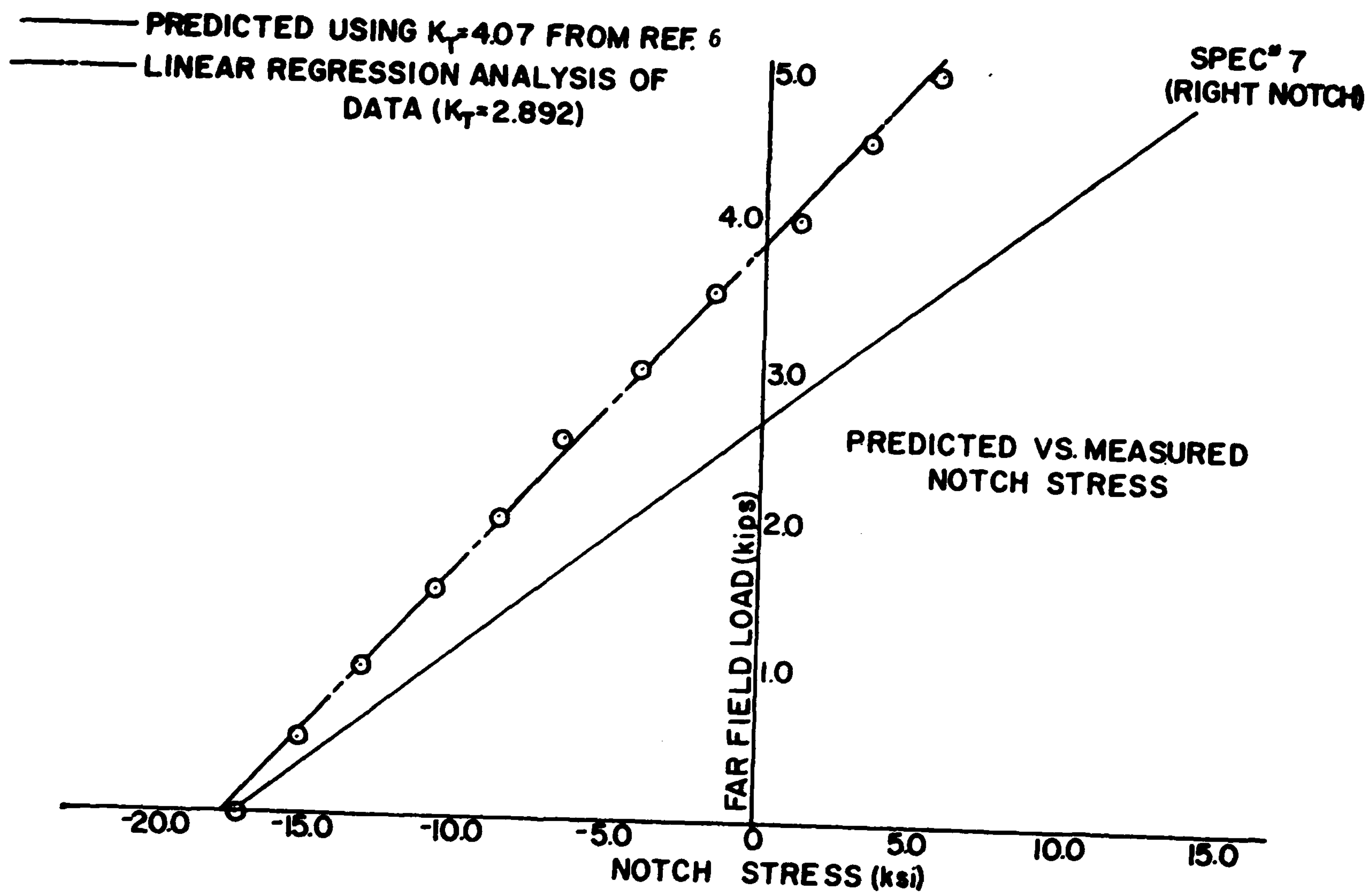

PREDICTED USING K_T=4.07 FROM REF. 6
LINEAR REGRESSION ANALYSIS OF DATA (K_T=2.892)
SPEC# 7
(RIGHT NOTCH)
PREDICTED VS. MEASURED NOTCH STRESS
5.0
4.0
3.0
2.0
1.0
FAR FIELD LOAD (kips)
-20.0
-15.0
-10.0
-5.0
0
5.0
10.0
15.0
NOTCH STRESS (ksi)

FIGURE 12

Using thin, perforated strips of a strain-hardening aluminum, Theocaris and Marketos [9] showed in 1964 that the value of K_T behaved in accordance with Hill's experiments. But, in addition, they showed an increase in K_ε with successively higher loadings for their strain-hardening material. Therefore, K_ε was calculated for each specimen at the σ_{MAX} loading condition of [6] and again for the higher σ_{MAX} loading condition of this thesis. Table 8 of Appendix A summarizes the results. The change in K_ε at the higher stress level ranged from 1.6% lower to 7.5% higher than for the lower stress level. This was about the same spread observed for the K_T reduction data; and, therefore, the change in K_ε was not considered to be significantly different from zero. The lack of any significant change in K_ε with higher stress levels as opposed to the findings of Theocaris and Marketos could be attributed to the near-perfect plastic behavior of the 7075-T6 aluminum as compared to the strain-hardening material used by Theocaris.

IV. CONCLUSIONS AND RECOMMENDATIONS

Cyclic loading did not appear to change the residual stress value appreciably. Eight different specimens with two different notch geometries were tested at peak load levels of from 7.90 kips to 15.96 kips up to 100,000 cycles. Each specimen had a different level of residual stress induced by Stuart [6]. Despite the differences in geometry, loading conditions, test duration, and previous history, the residual stress value remained immutable in every case.

The value of K_T appeared to decrease when the notch was subjected to plastic strain levels as reported in [8] and [9]. Three specimens were loaded to 18.00 kips in order to establish new levels of σ_{MAX} for use in the uniaxial model. This load was sufficiently great to cause plastic deformation in the region of the notch tips and thereby relax the concentration of the stress there [8]. Hence, when the original value of K_T was used to predict the notch stress for the low-load tests (up to 5.00 kips in 0.50 kip increments), the predicted notch stresses were significantly higher than measured photoelastically. The linear regression analyses of the data revealed that the K_T's must have been reduced an average of 23.9%. No correlation was established between the percent reduction at each notch and either the previous K_T load or the load history of the specimens.

Unlike the strain-hardening aluminum of [9], the 7075-T6 aluminum specimens showed no increase in K_ϵ with additional plastic deformation at the notch. A comparison between the K_ϵ which existed under Stuart's σ_{MAX} conditions and the higher σ_{MAX} conditions of this thesis revealed

no significant change. The 7075-T6 aluminum tensile specimens demonstrated almost perfectly plastic behavior beyond the elastic limit. This material behavior, contrasted with that of [9], could account for the difference in results.

Further work must be done to implement these findings into a notch stress prediction model for use with the forthcoming microprocessor data from the fatigue monitoring systems soon to be installed in operational aircraft.

APPENDIX A: EXPERIMENTAL DATA

Table 1

Uniaxial Tensile Test Results with Aluminum Type B Specimen

σ (ksi)	ϵ_{LE} (μs)	ϵ_{LG} (μs)	ϵ_{TG} (μs)	σ (ksi)	ϵ_{LE} (μs)	ϵ_{LG} (μs)	ϵ_{TG} (μs)
1.114	140	86	- 32	46.806	4,704	4,590	-1,514
2.244	240	190	- 67	49.094	4,944	4,817	-1,587
3.744	384	334	- 117	51.278	5,170	5,035	-1,657
4.710	478	428	- 148	53.492	5,398	5,256	-1,727
6.166	616	570	- 196	55.766	5,638	5,482	-1,799
7.459	742	696	- 239	58.039	5,876	5,708	-1,871
8.930	882	840	- 286	59.510	6,030	5,855	-1,917
11.219	1,108	1,066	- 361	61.784	6,266	6,081	-1,989
14.948	1,474	1,433	- 482	63.968	6,492	6,300	-2,058
16.568	1,630	1,593	- 535	65.989	6,704	6,503	-2,121
18.648	1,832	1,798	- 603	68.961	7,012	6,800	-2,214
20.758	2,048	2,006	- 672	70.060	7,134	6,912	-2,249
22.407	2,212	2,169	- 726	70.922	7,230	7,000	-2,276
24.532	--	2,379	- 794	73.017	7,456	7,211	-2,338
26.806	2,654	2,602	- 869	74.295	7,596	7,346	-2,381
29.034	2,876	2,823	- 940	76.019	7,848	7,559	-2,446
31.947	3,178	3,112	-1,034	76.851	8,374	8,148	-2,590
34.384	3,428	3,353	-1,114	78.272	9,404	9,287	-2,890
36.464	3,640	3,560	-1,181	78.782	9,596	9,480	-2,946
38.619	3,862	3,775	-1,251	80.224	14,276	(2)	-4,360
40.907	4,090	4,002	-1,325	81.620	20,896	--	-6,422
43.136	4,322	4,223	-1,396	0.000	12,678	--	-3,789
44.607	4,476	4,370	-1,443				

ϵ_{LE} = longitudinal strain by extensometer

ϵ_{LG} = longitudinal strain by strain gauge

ϵ_{TG} = corrected transverse strain by strain gauge

LINEAR REGRESSION: $\sigma = 0.009915\epsilon_{LE} + 0.198$ (R = 0.999916), $\sigma = 0.010110\epsilon_{LG} + 0.422$ (R = 0.999994)

NOTES: 1. Only the first column was used for linear regression.

2. Amplifier saturated.

Table 2

Poisson's Ratios for Type B Specimen

σ (ksi)	ν_1	ν_2
1.114	.3721	.2286
2.244	.3526	.2792
3.744	.3503	.3047
4.710	.3458	.3096
6.166	.3421	.3166
7.459	.3420	.3208
8.930	.3405	.3243
11.219	.3386	.3258
14.948	.3364	.3270
16.568	.3358	.3282
18.648	.3354	.3291
20.758	.3350	.3281
22.407	.3347	.3282
24.532	.3338	--
26.806	.3340	.3274
29.034	.3330	.3268
31.947	.3323	.3254
34.384	.3322	.3250
36.464	.3317	.3245
38.619	.3314	.3239
40.907	.3311	.3240
43.136	.3306	.3230
44.607	.3302	.3224
46.806	.3298	.3219
49.094	.3295	.3210
51.278	.3291	.3205
53.492	.3286	.3199
55.766	.3282	.3191
58.039	.3278	.3184
59.510	.3274	.3179
61.784	.3271	.3174
63.968	.3267	.3170
65.989	.3262	.3164
68.961	.3256	.3157
70.060	.3254	.3153
70.922	.3251	.3148
73.017	.3242	.3136
74.295	.3241	.3135
76.019	.3236	.3117
76.851	.3179	.3093
78.292	.3112	.3073
78.782	.3108	.3070
80.244	(1)	.3054
81.620	--	.3073
0.000	--	.2989

$$\nu_1 = \frac{|\epsilon_{TG}|}{\epsilon_{LG}} \qquad \nu_2 = \frac{|\epsilon_{TG}|}{\epsilon_{LE}}$$

NOTE: 1. Amplifier saturated.

Table 3

Tensile Test Data from PS-1C Photoelastic Material

STRESS (psi)	LONGITUDINAL STRAIN (in/in)	COMPENSATOR
346.4	0.00139	50
562.9	0.00201	76
779.3	0.00260	100
995.7	0.00313	120
1,212.1	0.00370	141
1,645.2	0.00487	185
2,077.9	0.00631	238

LINEAR REGRESSION ANALYSIS:

$\sigma = 358{,}043\epsilon - 139.6$

Correlation = 0.9989

$\epsilon = 0.0012362N + 0.00000996$

Correlation = 0.9997

Discarding non-zero intercepts,

$E = 358{,}043$ psi

$\alpha = 0.0012362$

Table 4

Comparison of No-Load Residual Compensator Readings

SPEC.	K_T TYPE	COMPENSATOR [REF. 6]	READINGS
1	3.8	27/29	35.5/(1)
3	3.8	19/11.5	17/9.5
7	3.8	22/20	(1)/(1)
6	3.8	89/90	65/87
8	3.8	28/26.5	32.5/30
9	3.8	59.5/57	59.5/42.5
10	3.8	91/98	87/86
11	3.8	95.5/85.5	80/52.5
3	2.6	58/43	62/27
7	2.6	75/84.5	84/91
12	2.6	27/22.5	101/96
13	2.6	49/59	54.5/66

NOTE: 1. No fringes visible.

Table 5

Residual Compensator Readings after Loading to 18.00 kips

SPEC.	K_T TYPE	COMPENSATOR READINGS
1	3.8	55.5/(1)
3	3.8	56.5/55.5
7	3.8	48/50

NOTE: 1. Not bonded.

Table 6

Cyclic Test Results

SPEC.	NOTCH TYPE ($K_{T\text{-NOM}}$)	LOAD RANGE (kips)	CYCLES	RESIDUAL COMPENSATOR (NOTE 1)
6	3.8	1.40-10.32	0	88.5/70.5
			18,000	88/70
			21,726	FAILED
8	3.8	1.40-7.90	10,000	36.5/34.5
			28,000	39/38
			40,000	39/38.5
			50,000	37.5/39
			70,000	37.5/38.5
			100,000	37/37.5
9	3.8	1.40-7.90	0	42/54
			10,000	42/54
			25,000	41/54
			32,990	41/51.5
			50,000	41/51
			68,000	42/51
			86,000	41/52
			100,000	40/51
10	3.8	1.40-10.32	0	81/80.5
			10,000	81/81
			20,000	82.5/81.5
			30,000	84/83
			48,000	84/82
			57,898	FAILED
11	3.8	1.40-7.90	31,962	54/86
			41,964	56/88.5
			51,965	59/97
			61,966	58.5/98
			71,967	59/98.5
			89,968	59.5/102
			101,000	61/100
7	2.6	1.40-13.54	0	84.5/87
			10,000	83.5/86
			20,000	82.5/85.5
			30,000	82/86
			40,000	82.5/85.5
			50,000	82.5/85.5
			60,000	82.5/85.5
			90,000	81/85.5
			100,000	81.5/85.5

Table 6

Cyclic Test Results

(Cot'd.)

13	2.6	1.40-12.00	0	52/62
			10,000	50/60
			20,000	50/59
			30,000	49.5/59.5
			40,000	50/59
			60,000	50/60
			70,090	50.5/60.5
			89,100	51/60
			100,000	51/60.5
14	2.6	1.40-15.96	0	63/33
			10,000	63.5/32.5
			20,000	63/31.5
			30,000	61.5/32
			33,043	FAILED

NOTE: 1. Left/Right

Table 7

Linear Regression Analysis Results for Variable K_T

SPEC.	K_T [Ref. 6]	Equation of Data	K_T	σ_R from Equation (7) (ksi)
1	4.23	$P_{FF} = 0.1903\sigma_N + 3.714$	3.290	-19.52
		$r^2 = 0.99815$		
3 (left)	4.10	$P_{FF} = 0.1923\sigma_N + 2.867$	3.255	-14.91
		$r^2 = 0.99890$		
3 (right)	4.19	$P_{FF} = 0.1888\sigma_N + 2.952$	3.316	-15.64
		$r^2 = 0.99957$		
7 (left)	4.11	$P_{FF} = 0.2089\sigma_N + 3.750$	2.997	-17.95
		$r^2 = 0.99946$		
7 (right)	4.07	$P_{FF} = 0.2165\sigma_N + 3.800$	2.892	-17.55
		$r^2 = 0.99929$		

Table 8

Results of K_ε *Comparison*

SPEC	P_{FF} (kips)	K_ε	P_{FF} (kips)	K_ε	% INCREASE IN K_ε
1	13.60	3.665	18.00	3.903	+ 6.1
3 (left)	14.00	3.632	18.00	3.810	+ 4.7
3 (right)	14.00	3.882	18.00	3.819	- 1.6
7 (left)	14.00	3.632	18.00	3.810	+ 4.7
7 (right)	14.00	3.525	18.00	3.810	+ 7.5

List of References

1. Topper, T. H., Wetzel, R. M., and Morrow, J., "Neuber's Rule Applied to Fatigue of Notched Specimens," *Journal of Materials*, March 1969

2. Schijve, J., *The Accumulation of Fatigue Damage in Aircraft Materials and Structures*, paper presented at the Symposium on Random Load Fatigue, Lyngby, Denmark, 13 April 1972

3. Rotvel, F., *On Residual Stresses During Random Load Fatigue*, paper presented at the Symposium on Random Load Fatigue, Lyngby, Denmark, 13 April 1972

4. Neuber, H., "Theory of Stress Concentration of Shear Strained Prismatic Bodies with Arbitrary Nonlinear Stress-Strain Law," *Journal of Applied Mechanics*, December 1961

5. Garske, J. C., *An Investigation of Methods for Determining Notch Root Stress from Far Field Strain in Notched Flat Plates*, Master's Thesis, United States Naval Postgraduate School, Monterey, California, September 1977

6. Stuart, G. L., *An Investigation of Residual Stress Characterization of 7075-T6 Aluminum for Application in Fatigue Analysis*, Master's Thesis, United States Naval Postgraduate School, Monterey, California, December 1978

7. Zandman, F., Redner, S., and Dally, J. W., *Photoelastic Coatings*, The Iowa State University Press and Society for Experimental Stress Analysis, 1977

8. Hill, R., "The Plastic Yielding of Notched Bars Under Tension," *Quarterly Journal of Mechanics and Applied Mathematics*, Vol. II, Part I, 1949

9. Theocaris, P. S., and Marketos, E., "Elastic-Plastic Analysis of Perforated Thin Strips of a Strain-Hardening Material," *Journal of Mechanics and Physics of Solids*, Vol. 12, pp. 377-390

Initial Distribution List

		No. Copies
1.	Defense Technical Information Center Cameron Station Alexandria, Virginia 22314	2
2.	Library, Code 0142 United States Naval Postgraduate School Monterey, California 93940	2
3.	Department Chairman, Code 67 Department of Aeronautics United States Naval Postgraduate School Monterey, California 93940	1
4.	Professor G. H. Lindsey, Code 67Li Department of Aeronautics United States Naval Postgraduate School Monterey, California 93940	1
5.	LCDR Edward C. Engle Naval Electronic Sys Com HQ (PME-106) Washington, D.C. 20360	1